Response of the Double Layer Capacitance of a High-Temperature Superconductor/Fluid Electrolyte Interface to the Onset of Superconductivity

Stephen R. Peck,[†] Larry S. Curtin,[†,#] John T. McDevitt,[†,‡] Royce W. Murray,*[,†] James P. Collman,[§] William A. Little,[§] T. Zetterer,[∥] H. M. Duan,[⊥] C. Dong,[⊥] and A. M. Hermann[⊥]

Contribution from the Kenan Laboratories of Chemistry, The University of North Carolina, Chapel Hill, North Carolina 27599-3290, Department of Chemistry and Physics, Stanford University, Stanford, California 94305, Institute of Applied Physics, University of Regensburg, Regensburg, Germany, and Department of Physics, University of Colorado, Boulder, Colorado 80309-0390. *Received February 24, 1992*

Abstract: Measurements of interfacial (double layer) capacitance, C_{DL}, and charge transfer resistance, R_{CT}, have been made as a function of temperature at fluid electrolyte interfaces with electrodes made from two different Tl-based high-temperature superconductor materials. Measurements spanning the 112–119 K superconducting transition temperatures, T_c, of the HTSC electrodes reveal a smooth decrease in C_{DL} with decreasing temperatures, except that an abrupt, ca. 1 deg wide change in the shape of the C_{DL} vs temperature curve occurs at the T_c of the electrode. These are the first data which show that the onset of superconductivity can be reflected in a chemical phenomenon at a molecular fluid/HTSC interface. Of the several contributors to interfacial capacitance, it is hypothesized that alteration in charge carrier distribution or polarizability over the outermost electrode lattice layer as electron pairs start to appear at T_c is the most likely origin of the T_c-correlated capacitance feature. Alterations in the charge transfer resistance for electrochemical solvent reduction appear over the same temperature interval as the capacitance feature, but not as consistently.

Following the discoveries of a number of high-temperature superconductor phases beginning with that by Bednorz and Müller in 1986,[1] our laboratory became interested[2] in whether electrochemical experiments with these intriguing materials might reveal special phenomena associated with the interface between a superconducting electrode phase and a fluid molecular phase. Of particular interest is how the properties of superconductor/molecular interfaces differ depending on whether the temperature is less or greater than the transition temperature (T_c) of the superconductor phase. Electrochemical techniques that are sensitive to interfacial properties, such as capacitance and charge transfer resistance, are experimentally applicable to this problem, given a suitably ionically conducting fluid electrolyte solution. To this end, we have developed a low-temperature fluid electrolyte phase[3] which is a 2:1 v:v mixture of ethyl chloride and butyronitrile with 0.1–0.2 M Bu_4NClO_4 or Bu_4NPF_6 electrolyte, procedures for fashioning electrodes from the high-temperature superconductor (HTSC) materials,[2] and an experimental protocol to prepare superconductor interfaces with reasonably stable electrochemical properties.[2]

In this paper, we apply these materials[2,3] and procedures along with electrochemical impedance spectroscopy[4] to measure the interfacial (double layer) capacitances and charge transfer resistances of electrodes made from two different Tl-based HTSC's, at temperatures which span their T_c (*zero resistance*) values of 112 and 119 K. We will show that the interfacial capacitance responds to the onset of superconductivity in the electrode side of the interface by a change in the shape of the interfacial capacitance–temperature curve that occurs highly reproducibly over a 0.5–1-deg temperature interval, immediately below T_c. Abrupt changes in curve shape are also seen in plots of the charge transfer resistance for the electrochemical reduction of solvent vs temperature, but the reproducibility of these changes and of their correlation with T_c is less clear-cut.

We had (intuitive) reason to anticipate a special effect of superconductivity onset on the electrode/electrolyte solution interfacial capacitance. The capacitance of an electrode/fluid electrolyte interface is, in electrical equivalent terms, a series of capacitive charge-storing phenomena:[5,6] molecular dipole orientation and electrolyte ion adsorption at the solution/electrode interface (the solution part of the compact layer capacitance), a space charge of ions in the immediately adjacent solution (the diffuse layer capacitance), and the electronic charge carrier distribution over the outermost layer of atoms of the electrode[7]

[†] The University of North Carolina.
[#] Present address: Department of Chemistry, Temple University, Philadelphia, PA 19122.
[‡] Present address: Department of Chemistry and Biochemistry, The University of Texas, Austin, Texas 78712.
[§] Stanford University.
[∥] University of Regensburg.
[⊥] University of Colorado.

(1) (a) Bednorz, J. G.; Müller, K. A. *Z. Phys. B* **1986**, *64*, 189–193. (b) Wu, K. M.; Ashburn, J. R.; Torng, C. J.; Hor, P. H.; Meng, R. L.; Gao, L.; Huang, Z. J.; Wang, Y. Q.; Chu, C. W. *Phys. Rev. Lett.* **1987**, *58*, 908.
(2) (a) McDevitt, J. T.; McCarley, R. L.; Dalton, E. F.; Gollmar, R.; Murray, R. W.; Collman, J. P.; Yee, G. T.; Little, W. A. In *Chemistry of High-Temperature Superconductors II*; Nelson, D. L., George, T. F., Eds.; ACS Symposium Series 377; American Chemical Society: Washington, DC, 1988; pp 207–222. (b) McDevitt, J. T.; Longmire, M.; Gollmar, R.; Jernigan, J. C.; Dalton, E. F.; McCarley, R. L.; Murray, R. W.; Little, W. A.; Yee, G. T.; Holcomb, M. J.; Hutchinson, J. E.; Collman, J. P. *J. Electroanal. Chem. Interfacial Electrochem.* **1988**, *243*, 465–474. (c) McDevitt, J. T.; Shah, S. I.; Murray, R. W. *J. Electrochem. Soc.* **1991**, *138*, 1346–1350. (d) Gollmar, R.; McDevitt, J. T.; Murray, R. W. *J. Electrochem. Soc.* **1989**, *136*, 3696–3701.
(3) (a) McDevitt, J. T.; Ching, S.; Sullivan, M.; Murray, R. W. *J. Am. Chem. Soc.* **1989**, *111*, 4528–4529. (b) Ching, S.; McDevitt, J. T.; Peck, S. R.; Murray, R. W. *J. Electrochem. Soc.* **1991**, *138*, 2308–2315.
(4) (a) Macdonald, J. R., Ed. *Impedance Spectroscopy*; Wiley-Interscience: New York, 1987. (b) Sandifer, J. R.; Buck, R. P. *J. Electroanal. Chem. Interfacial Electrochem.* **1974**, *56*, 385–378. (c) Bruce, P. G. *Polymer Electrolyte Reviews 1*; MacCallum, J. R., Vincent, C. A., Elsevier Science: New York, 1987; pp 237–274.
(5) Bard, A. J.; Faulkner, L. R. *Electrochemical Methods*; Wiley: New York, 1980.
(6) Parsons, R. *Chem. Rev.* **1990**, *90*, 813–826.
(7) (a) Price, D.; Halley, J. W. *J. Electroanal. Chem. Interfacial Electrochem.* **1983**, *150*, 347–353. (b) Halley, J. W.; Johnson, B.; Price, D.; Schwalm, M. *Phys. Rev. B* **1985**, *31*, 7695–7709. (c) Schmickler, W. *J. Electroanal. Chem. Interfacial Electrochem.* **1983**, *150*, 19–24. (d) Schmickler, W.; Henderson, D. *J. Chem. Phys.* **1984**, *80*, 3381–3386. (e) Schmickler, W.; Henderson, D. *J. Chem. Phys.* **1986**, *85*, 1650–1657. (f) Badiali, J. P.; Rosinberg, M. L.; Goodisman, J. *J. Electroanal. Chem. Interfacial Electrochem.* **1981**, *130*, 31–45. (g) Badiali, J. P.; Rosinberg, M. L.; Goodisman, J. *J. Electroanal. Chem. Interfacial Electrochem.* **1983**, *143*, 73–88. (h) Badiali, J. P.; Rosinberg, M. L.; Goodisman, J. *J. Electroanal. Chem. Interfacial Electrochem.* **1983**, *150*, 25–31. (i) Amokrane, S.; Russier, V.; Badiali, J. P. *Surf. Sci.* **1989**, *210*, 251–270. (j) Amokrane, S.; Badiali, J. P. *J. Electroanal. Chem. Interfacial Electrochem.* **1989**, *266*, 21–35. (k) Amokrane, S.; Badiali, J. P. *Electrochim. Acta* **1989**, *34*, 39–45.

0002-7863/92/1514-6771$03.00/0

(the electrode part of the compact layer capacitance). The (reciprocally) summed, overall capacitance is called[5] the double layer capacitance, C_{DL}. Since the superconductivity phenomenon leads to an alteration of the electronic charge carriers, i.e., the formation of paired electron states, we hypothesized that the electrode capacitance component of the HTSC electrode double layer might be observably altered at temperatures at or below T_c.

Analogous questions have also been explored by Lorenz et al.[8] at several HTSC/silver β''-alumina interfaces. Using this *solid* electrolyte, these workers discovered the first example of an electrochemical response to the onset of electrode superconductivity, correlating changes in charge transfer resistance and in associated interfacial capacitance with the T_c of the solid-state assembly. Others, including electron transfer theorists, have also contributed.[9] The experimental observations presented here comprise the first evidence that *fluid molecular* interfaces also respond to the onset of superconductivity. Fluid molecular interfaces offer advantages of better contact with the superconductor phase and a greater ultimate diversity of molecular charge transfer systems than do solid–solid interfaces.

Experimental Section

Chemicals. Butyronitrile (PrCN, Aldrich, 99+%) was distilled from CaH_2 under N_2. Ethyl chloride (EtCl, Linde) was condensed into a Schlenk tube and stored at room temperature (vapor pressure ca. 1.5 atm). Tetra-*n*-butylammonium perchlorate (Bu_4NClO_4) was prepared from Bu_4NBr and perchloric acid and twice recrystallized from ethyl acetate.[10] Sintered pellets whose X-ray diffraction patterns indicated predominantly $Tl_2Ba_2Ca_2Cu_3O_{10}$ (Tl-2223) phase[8,11] and roughly equal proportions of $Tl_2Ba_2CaCu_2O_8$ (Tl-2212) and Tl-2223 phases[12] were prepared by literature methods and their T_c values (112 and 119 K, respectively) established (for zero resistance) by resistivity measurements. For simplicity, we label these T_c = 112 and 119 K samples as Tl_{2223} and Tl_{2212}, respectively.

Electrode Fabrication. The sintered pellets of Tl_{2223} and Tl_{2212} were cleaved into ~2-mm blocks with a razor blade. Electrical contact was made by vapor depositing approximately 0.3 μm of silver onto one face of the superconductor electrode; a Ag-coated Cu wire was attached to this pad with silver solder (Kester) and reinforced with a bead of silver epoxy (Epoxy Technology Inc., epo-Tek H2OE, cured overnight at 70 °C). The superconductor working electrode and a 0.5 mm diameter silver wire (quasi-reference electrode) were placed in a cylindrical mold which was evacuated before introducing an insulating epoxy (Shell EPON 828, *m*-phenylenediamine curing agent, cured overnight at 70 °C). The end of the resulting (6 mm diameter, ca. 5 cm long) epoxy-encapsulated superconductor assembly was sanded (Buehler 600 grit) to expose the superconductor working and Ag reference electrodes.

Prior to each experiment, fragments from the superconductor surface were cleaved away under N_2 atmosphere in a drybox to provide a pristine surface. We have established that such freshly exposed superconductor surfaces exhibit[2] good room-temperature electrochemical electron transfer properties. The cylindrical working and reference electrode assembly fit into a stainless steel cylinder with a platinum disk counter electrode bottom, providing a cofacial working/counter electrode orientation.

Pt and glassy carbon working electrodes used as control materials were prepared by a similar procedure and used in the same cell geometry.

Impedance Measurements. In electrochemical impedance spectroscopy, a constant-amplitude sinusoidal voltage, centered at a dc bias voltage (relative to the reference electrode), is applied to the working electrode. The resulting sinusoidal current amplitude and phase angle, ϕ, with respect to the voltage perturbation are measured at a succession of different frequencies using a frequency response analyzer (Schlumberger-Solartron Instruments Model 1255) and a potentiostat (Schlumberger-Solartron Instruments Model 1286) under computer control (Zenith). The amplitude and phase angle of the current are characteristic of the impedance of the cell and are presented as an impedance (or Nyquist) plot of imaginary (90° out-of-phase, Z'') vs real (in-phase, Z') impedances. Each data point on such plots represents a different frequency.

Experimental Procedure. Sufficient ethyl chloride was added to a Bu_4NClO_4/butyronitrile solution at dry ice temperature to prepare a 0.1–0.2 M Bu_4NClO_4/2:1 v:v EtCl:PrCN solution. A fresh surface of the superconductor electrode was exposed by cleaving the superconductor with a razor blade in a nitrogen atmosphere glove box and transferring the freshly cleaved electrode to the cold electrolyte solution. The cell was adjusted so that the counter and working electrodes were separated by ca. 100 μm and was placed in a liquid nitrogen cryostat (Janis Model 6CND-NVT, equipped with a Lakeshore Model 805 temperature controller, maintains temperatures to ±0.1 K). After the temperature was brought to the desired initial value, usually between 120 and 130 K, and thermal equilibrium was established, current and phase angle measurements were performed over a frequency range of typically 10 kHz–0.01 Hz to acquire the impedance spectrum. During the experiment, the impedance spectrum was evaluated at a succession of gradually lowered temperatures. Additionally, at least two measurements of the complete impedance frequency spectrum were taken at most temperatures, to check for reproducibility of the derived R and C values, which was typically 1–2% (RSD). Experiments in which poor reproducibility was encountered (sometimes a consequence of very large solution resistance) were aborted and are not reported here. A voltage perturbation of 1000 mV was required to produce measurable currents at temperatures below 130 K. While larger than desirable, perturbations of several volts are common for ultralow-temperature, very high impedance measurements.[8,13]

The dc voltage bias applied to Tl_{2223} working electrodes was typically −3.5 V vs Ag quasi-reference electrode. This voltage promotes a reduction reaction that we presume is the reduction of a solvent component, probably that of ethyl chloride. The other dc bias voltages (all vs Ag) are for Tl_{2212}, −2.5 to −3.5 V, for glassy carbon, −2.0 to −3.0 V, and for platinum, −2.0 to −3.0 V. These voltages were selected to give comparable Nyquist plots for the different electrode materials.

Impedance Data Analysis. The impedance data were fit to an equivalent circuit (representing the electrochemical cell)[4] using a Marquardt–Levenberg nonlinear least squares routine. The equivalent circuit employed consists of two parallel RC circuits, in series, one representing the parallel solution resistance and capacitance and the other the parallel charge transfer resistance and double layer capacitance of the working electrode/solution interface:

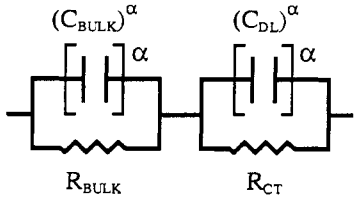

This equivalent circuit, while not the only possible representation, has frequently been employed[4b,c] to represent electrochemical interfaces and, in the present case, provided the best fit to the data. The capacitances

(8) (a) Pinkowski, A.; Jüttner, K.; Lorenz, W. J. *J. Electroanal. Chem. Interfacial Electrochem.* **1990**, *287*, 203–213. (b) Pinkowski, A.; Jüttner, K.; Lorenz, W. J.; Saemann-Ischenko, G.; Breiter, M. W. *J. Electroanal. Chem. Interfacial Electrochem.* **1990**, *286*, 253–256. (c) Pinkowski, A.; Doneit, J.; Jüttner, K.; Lorenz, W. J.; Saemann-Ischenko, G.; Zetterer, T.; Breiter, M. W. *Electrochim. Acta* **1989**, *34*, 1113–1117. (d) Pinkowski, A.; Doneit, J.; Jüttner, K.; Lorenz, W. J.; Saemann-Ischenko, G.; Zetterer, T.; Breiter, M. W. *Physica C* **1989**, *162–164*, 1039–1040. (e) Bachtler, H.; Lorenz, W. J.; Schindler, W.; Saemann-Ischenko, G. *J. Electrochem. Soc.* **1988**, *135*, 2284–2287. (f) Pinkowski, A.; Lorenz, W. J.; Saemann-Ischenko, G. *Solid State Ionics* **1990**, *40/41*, 822–824. (g) Pinkowski, A.; Doneit, J.; Jüttner, K.; Lorenz, W. J.; Saemann-Ischenko, G.; Breiter, M. W. *Europhys. Lett.* **1989**, *9*, 269–276. (h) Breiter, M. W.; Lorenz, W. J.; Saemann-Ischenko, G. *Surf. Sci.* **1990**, *230*, 213–221. (i) Lorenz, W. J.; Saemann-Ischenko, G.; Breiter, M. W. *Ber. Bunsen-Ges Phys. Chem.* **1991**, *95*, 1055–1061.

(9) (a) Bockris, J. O'M.; Wass, J. *J. Electroanal. Chem.* **1989**, *267*, 329–332. However see also the following references: (b) Rosamilia, J. M.; Miller, B.; Schneemeyer, L. F.; Waszczak, J. V.; O'Bryan, H. M., Jr. *J. Electrochem. Soc.* **1987**, *134*, 1863–1864. (c) Magee, V. M.; Rosamilia, J. M.; Kometani, T. Y.; Schneemeyer, J. F.; Waszczak, J. V.; Miller, B. *J. Electrochem. Soc.* **1988**, *135*, 3026–3030. (d) Kuznetzov, A. M. *J. Electroanal. Chem. Interfacial Electrochem.* **1990**, *278*, 1–15. (e) Zusman, L. D.; Gelman, A. B.; Shapiro, B. Ya. *Chem. Phys. Lett.* **1990**, *167*, 457–459.

(10) Sawyer, D. T.; Roberts, J. L., Jr. *Experimental Electrochemistry for Chemists*; Wiley-Interscience: New York, 1974; p 212.

(11) (a) Zetterer, T.; Otto, H. H.; Lugert, G.; Renk, K. F. *Z. Phys. B: Condens. Matter* **1988**, *73*, 321–328. (b) Otto, H. H.; Zetterer, T.; Renk, K. F. *Naturwissenschaften* **1988**, *75*, 509–510. (c) Zetterer, T.; Ose, W.; Schutzmann, J.; Otto, H. H.; Obermayer, P. E.; Tasler, N.; Lengfellner, H.; Lugert, G.; Keller, J.; Renk, K. F. *J. Opt. Soc. Am. B* **1989**, *6*, 420–435. (d) Zetterer, T.; Franz, M.; Schutzmann, J.; Ose, W.; Otto, H. H.; Renk, K. F. *Phys. Rev. B* **1990**, *41*, 9499–9501.

(12) (a) Sheng, Z. Z.; Hermann, A. M. *Nature* **1988**, *332*, 138–139. (b) Sheng, Z. Z.; Kiehl, W.; Bennett, J.; El Ali, A.; Marsh, D.; Mooney, G. D.; Arammash, F.; Smith, J.; Viar, D.; Hermann, A. M. *Appl. Phys. Lett.* **1988**, *52*, 1738–1740.

(13) Cappadonia, M.; Stimming, U. *J. Electroanal. Chem. Interfacial Electrochem.* **1991**, *300*, 235–248.

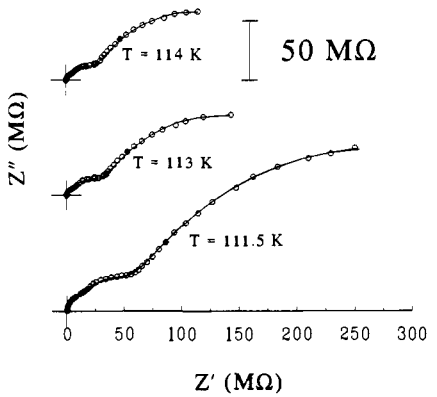

Figure 1. Nyquist impedance plots (crosses denote origins) for a Tl_{2223} working electrode obtained at 114 K (top), 113 K (middle), and 111.5 K (bottom): o, experimental data; solid lines, Marquardt–Levenberg data fits for equivalent circuits comprising two parallel RC circuit elements. The plot for 111.5 K also shows a fit for three RC circuit elements; the two- and three-element fits (see text) differ at high but not at low frequency. The ● in each plot indicates the data point at 0.1 Hz. $E_{app,dc}$ = −3.5 V vs Ag, ΔE_{ac} = 1000 mV, and frequency range = 10^4–10^{-2} Hz from left to right.

are represented by a constant phase element, which more accurately accounts for geometrical nonidealities such as surface roughness and nonuniform current densities.[4,14] The impedance, Z, of each distributed element RC circuit is given by

$$Z = \frac{R}{1 + RC(j\omega)^{\alpha}} \qquad (1)$$

where R and C are resistance and capacitance, ω is the frequency (rad/s), and $j = \sqrt{-1}$. The exponent α is unity for an ideal capacitor; however, in the electrochemical cells employed here, α values between 0.6 and 0.8 produced the best fits in the low frequency region of the impedance spectrum.

Two semicircular arcs are expected in the impedance (Nyquist) plots for the above equivalent circuit. Occasionally we observe Nyquist plots at HTSC electrodes in which the higher frequency (left-hand) arc separates into two arcs, the highest frequency one being generally quite small (see Figure 1, T = 111.5 K). This behavior is also typical for glassy carbon electrodes. Recent refinements in the wiring between the cryostat cell and impedance analyzer have made this effect less pronounced, and we accordingly suspect that it is associated with stray capacitance. This third arc, when present, is represented with a third distributed element RC circuit, in series with the above two, but this in fact is not an important step, since the analysis of the low frequency results for C_{DL} and R_{CT} *changes by <10% in absolute magnitude and not at all in the shape of the temperature dependence* whether the third RC element is included in the equivalent circuit or is ignored.

T_c Post-Mortem. To ensure that the Tl_{2223} superconductor retained its conductive and superconductive properties following use as an electrode, its T_c was determined following a complete set of low-temperature impedance measurements. The determination was carried out as a four-probe resistivity measurement by applying four parallel lines of conducting silver paint (SPI Systems) to the exposed face of the used electrode. A wire was attached to each line with silver epoxy, and the electrode was returned to the cryostat. A Keithly Model 224 programmable current source impressed a current (typically 10 mA) through the two outer contacts, and the voltage drop between the inner contacts was measured as a function of temperature with a Keithly Model 197 digital multimeter.

Results and Discussion

Impedance Analysis. Plots of in-phase and out-of-phase impedances (Nyquist plots) determined using a Tl_{2223} electrode in the low-temperature fluid electrolyte system are shown in Figure 1. Note that the temperatures employed span the superconducting transition temperature of the electrode material and that *the lower curve corresponds to the interfacial impedance characteristics of an interface between a superconducting and a fluid (normal) molecular phase.* These are the first such data, for molecular materials, of which we are aware.

The Nyquist plots in Figure 1 (and those at higher and lower temperatures) reveal a strong relation between the values of impedance and temperature. A detailed analysis of the impedance results is required, however, to ascertain whether any special change occurs at the temperature of onset of electrode superconductivity.

The Nyquist plots in Figure 1 exhibit three arcs, the highest frequency one of which is quite small and often difficult to see and is thought to be associated with stray capacitance. In the figure, the data points decrease from high to low frequency from left to right. The arcs in Figure 1 are modeled as a series of two parallel RC elements (vide supra); nonlinear least squares fitting (solid line) of the data (open circles) with eq 1 typically produced excellent fits, especially over the lower frequency arc. A fit using three RC elements is also shown for T = 111.5 K to illustrate that this detail does not affect fitting of the data in the most important (vide infra) low frequency regime. Interpretation of the low frequency data yields results for the electrode double layer capacitance and charge transfer resistance.

To fit the experimental data to theoretical curves, the initial calculations were performed with floating R, C, and α parameters for all of the RC circuit elements. The exponent α varied randomly by a few percent with temperature. The major contributor to α was probably the roughness of the cleaved electrode surfaces,[14] which should not change with temperature. Data were refit therefore using the average α for that electrode; there were only minor differences in R and C values obtained in the initial and refined fitting steps.

In order to establish which of the impedance arcs represent the electrode/solution interface, Nyquist plots were obtained as a function of dc bias voltage. The low frequency (right-hand) arc was extremely sensitive to applied bias voltage whereas the high frequency arcs were completely unresponsive. Thus, the low frequency arc represents the interfacial impedance and the (major) high frequency arc the electrolyte solution impedance.[15] As expected, at more negative bias voltages, the resistive (R_{CT}) component of the low frequency arc becomes smaller, since the charge transfer resistance of the electrochemical reaction at the superconductor/electrolyte interface should become smaller (i.e., faster kinetics) at higher voltage driving forces.[16] The normally expected exponential dependence of charge transfer resistance on potential could not be carefully evaluated, being smeared by the large ac voltage perturbation that, for signal/noise reasons, was necessary to employ.

In contrast to the behavior of the low frequency resistive elements, the capacitance obtained from the low frequency arc varied only mildly with the applied dc potential bias. Double layer capacitances in general are not expected to vary strongly with electrode potential. Given all these facts, we conclude that the low frequency arc represents the parallel combination of interfacial impedances, the resistance to charge transfer (R_{CT}) and double layer capacitance (C_{DL}), whose values we seek to measure as a function of temperature.

Double Layer Capacitance Results. Plots of C_{DL}, normalized to geometrical electrode area, vs temperature are shown in Figure 2a–c for a series of experiments using different Tl_{2223} electrodes with a dc bias of −3.5 V vs Ag. The absolute magnitudes of the double layer capacitances, C_{DL}, of the different electrodes vary due to uncertainty in the microscopic area, but the shapes of the plots in Figure 2a–c are similar in that they all display an abrupt, 0.5–1 deg wide change in the shape of the C_{DL} vs temperature plot just below the T_c for this material. The change in shape appears as an abrupt flattening of the slope with which interfacial capacitance decreases with temperature; Figure 2a exemplifies this feature, which was always present in the capacitance curve

(14) Maritan, A.; Toigo, F. *Electrochim. Acta* **1990**, *35*, 141–145.

(15) The bulk impedance of the electrode material itself, including in the normal ($T > T_c$) state, is completely insignificant on the scale of impedances in Figure 1.

(16) For example, a glassy carbon electrode at 120 K gave charge transfer resistances (from the low frequency arc) varying (roughly) exponentially from 21 MΩ at E = −1.5 V vs Ag to 2.3 MΩ at E = −3.0 V vs Ag. Qualitatively similar results were also observed at superconductor and platinum electrodes.

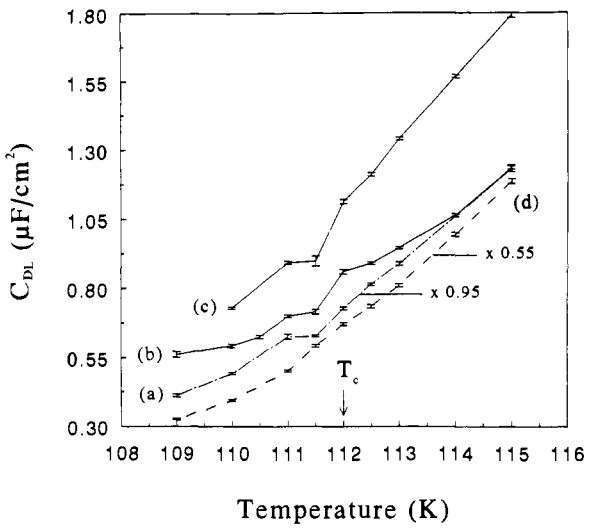

Figure 2. Temperature dependence of C_{DL} obtained from the low frequency arc in plots like those in Figure 1, normalized for geometrical electrode area: curves a–c, Tl_{2223} electrodes ($E_{app,dc}$ = −3.5 V vs Ag); curve d, glassy carbon electrode ($E_{app,dc}$ = −2.0 V vs Ag). Curves a and d are scaled differently for clarity of presentation. Data points are at the centers of the 2σ wide error bars.

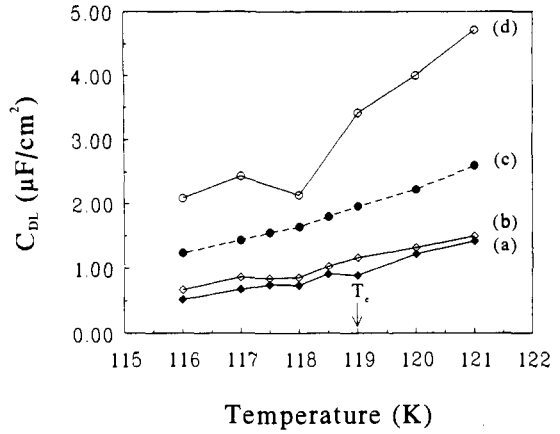

Figure 3. Temperature dependence of C_{DL}: curves a, b, and d, Tl_{2212} electrodes ($E_{app,dc}$ = −3.5, −3.0, and −2.5 V vs Ag, respectively); curve c, glassy carbon electrode ($E_{app,dc}$ = −3.0 V vs Ag). (Error bars if shown would be smaller than the data symbols.)

shape change. Additionally, in about half of the C_{DL}–temperature runs, just prior to the flattening, an initially steeper decrease in capacitance also occurs, as seen in Figure 2b,c. Both effects yield the visual appearance of a dip in the capacitance curve just below T_c. The steep capacitance decrease amounts to a 10–30% drop in C_{DL} over a 0.5 K interval, which is a very substantial change. (The change observed in C_{DL} in the analogous superconductor/solid electrolyte experiments[8a] was also quite abrupt and transitory, but of smaller magnitude.) The variability in the appearance of the capacitance curve shape changes (flattening vs dip) must reflect some uncontrolled variability in the nature of the cleaved HTSC electrode surface.

That the observed dip in double layer capacitance is associated with the onset of electrode superconductivity was confirmed by experiments with electrodes of a different stoichiometry and T_c. Impedance measurements performed on Tl_{2212} superconductor electrodes gave the C_{DL} vs temperature plots shown in Figure 3a,b,d for three different Tl_{2212} electrode samples at three different bias voltages. All show a dip-like curve shape change just below T_c, irrespective of the bias voltage used.[17]

We should emphasize that while the T_c-correlated changes in the shape of the capacitance–temperature curves in Figures 2 and 3 are relatively small effects, the statistics of the collected data and their analysis demonstrate that the shape changes are real. The magnitudes of the shape changes in double layer capacitance at T_c are well outside the experimental uncertainty of the individual C_{DL} data points. The relative standard deviations of the data points in Figures 2 and 3 as obtained from the impedance analysis fits are typically 1–2%; error bars shown in Figure 2 are insignificant on the scale of the observed changes in C_{DL}. Multiple impedance spectra were routinely collected at each temperature setting during a capacitance–temperature experiment and were similarly reproducible. The influence of details of the impedance analysis on the T_c-related capacitance features in Figures 2 and 3 was also examined with great care. The use, for example, of different values of the parameter α produces small changes in the absolute magnitude of C_{DL} but does not affect the appearance of the dip. The capacitance curve shape change at T_c was furthermore observed for many more electrode samples than those whose curves are shown in Figures 2 and 3, in fact in a total of 14 out of 15 capacitance–temperature runs (11 with Tl_{2223} and 4 with Tl_{2212}) in which we were successful in accurately measuring capacitance at 0.5–1 K intervals over a 6–7 K span centered around T_c. Only one such experiment did not show a clear feature at T_c in the C_{DL} vs temperature curve. Six experiments showed the capacitance feature only as a flattening of the slope of the capacitance curve just below T_c (e.g., Figure 2a); eight others additionally displayed the steeper slope before the flattening (e.g., Figures 2b,c and 3d). The ratios of the slopes of capacitance–temperature curves *above* T_c to those in the flattened interval just *below* T_c averaged to 2.2 ± 1.3, not including the results for two samples whose slope ratios were much larger (53 and 207). For the samples displaying the more obvious dip, the ratios of the slopes of the capacitance–temperature curves observed *above* T_c to those in the steeper-slope interval just *below* T_c averaged to 0.6 ± 0.1.

To ensure that the dips in C_{DL} are not caused by an artifact associated with the experimental method or the solvent system, C_{DL} was also measured at glassy carbon electrodes (a non-superconductor) over the same temperature intervals as in Figures 2 and 3. The results are shown as Figures 2d and 3c. In both cases, C_{DL} decays smoothly, with no dip, past the relevant T_c temperatures. Similar results are obtained using Pt control electrodes.

We regard the preceding data as firm evidence for an abrupt change in the temperature dependency of the double layer capacitance of a superconductor/fluid electrolyte interface as the superconductor undergoes transition from a normal to a superconducting state. Obtaining such evidence, the first of its kind, was the principal objective of this study.

The double layer capacitance of an electrode/electrolyte interface is not governed by any single interfacial property but, as noted above, reflects the polarizability or charge-storing capacity of several interfacial phenomena. One of these is the ionic space charge (diffuse) layer[5] which is electrostatically established in the solution next to the interface. We believe it unlikely that the appearance of electron pairs in the electrode at T_c would influence the diffuse layer capacitance, since the diffuse layer is separated from the electrode by a layer of solvent dipoles which are part of the so-called compact layer capacitance. The compact layer capacitance is currently understood[6,7] as having two charge-storing components, one being on the solution side of the interface and consisting of solvent dipole reorientations and adsorption of electrolyte ions at the electrode/solution interface and the other involving the distribution and polarizability of charge carriers positioned on the outermost atomic lattice layer of the electrode material (the electrode part of the compact capacitance). We know of no theoretical basis for distinguishing between the sensitivity of these two charge-storing mechanisms to the onset of superconductivity. However, the electrode part of the compact layer capacitance is known[6,7] to be sensitive to the electronic properties of the electrode material and differs for a given metal according to the crystal plane exposed. Current explanations[6,7]

(17) Any dependency of the dip in C_{DL} on dc voltage bias may be obscured by the large ac voltage perturbation employed. The fluctuations in the absolute values of C_{DL} are probably associated with differing microscopic area rather than potential dependency.

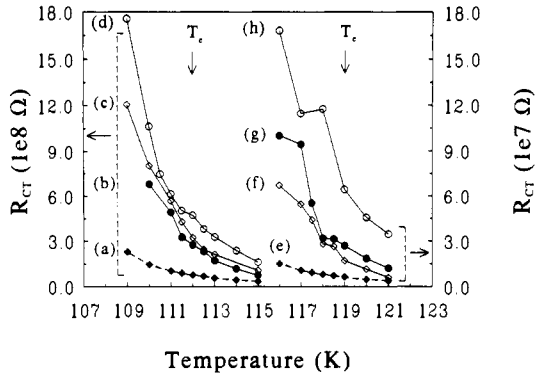

Figure 4. Temperature dependence of R_{CT}: curves b–d, Tl_{2223} electrodes ($E_{app,dc}$ = −3.5 V vs Ag); curves f–h, Tl_{2212} working electrodes ($E_{app,dc}$ = −3.5, −3.0, and −2.5 V vs Ag, respectively); curves a and e, glassy carbon working electrodes ($E_{app,dc}$ = −2.0 and −3.0 V vs Ag, respectively). Curves b and f are lowered by 30 and 11 MΩ, respectively, for clarity of presentation.

of the electrode part of the compact layer capacitance are based upon an outer atomic layer charge distribution model. It seems reasonable therefore to speculate that a change in the electrode (surface) part of the compact layer capacitance is the likely origin of the capacitance curve shape effects observed in Figures 2 and 3. This speculation would imply that either the polarizability or the distribution of charge carriers over the outermost HTSC electrode lattice layer is changed at T_c by the appearance of electron pairs there as part of the charge carrier population.

Unraveling the contributions of individual interfacial phenomena to double layer capacitances has classically been difficult. In ongoing studies of the HTSC electrode/fluid electrolyte interface, we are attempting to manipulate the capacitance of the solution side of the interface. Since C_{DL} is a reciprocal sum of the above capacitances, an increase in the solution capacitance term should enhance the effect of the electrode capacitance on C_{DL}. It is possible then that effects larger than those seen in Figures 2 and 3 might be elicited in future experiments.

Charge Transfer Resistance Results. Working at solvent-reducing potentials also afforded the opportunity to examine possible changes in charge transfer resistance (R_{CT}) as the electrode becomes superconducting. Plots of R_{CT} vs temperature for the same electrodes and under the same experimental conditions as used in Figures 2 and 3 are shown in Figure 4. Parts b and f of Figure 4 are offset by 30 and 11 MΩ, respectively, for clarity of presentation. These data, like the C_{DL} results, have RSD values of 1–2%. The charge transfer resistances increase steadily with decreasing temperatures, as expected for an activated reaction. The data are tantalizing because sharp changes are evident in some of the curves in the vicinity of T_c, and these sharp changes are not seen at glassy carbon electrodes (Figure 4a,e). Whether the kinetics of electron transfer are altered when a superconducting interface delivers the electrons (or electron pairs) is of course a question of fundamental significance. We note that the electrode reaction involved is probably the reduction of ethyl chloride. However, careful examination of the results suggests caution. The sharp changes in R_{CT} are not as consistently at the same temperature with respect to T_c as are the C_{DL} results, and in 4 of the 15 experimental runs, the change either was minor (i.e., Figure 4c) or was within experimental uncertainty. We choose at present to be conservative and say that these charge transfer data are provocative but, in contrast to the double layer capacitance results, are not conclusive.

Table I. Typical Values of R_{bulk} and C_{bulk} as a Function of Temperature

T (K)	R_{bulk} (MΩ)	C_{bulk} (μF/cm²)
115	8.1	0.143
114	11.3	0.124
113	16.4	0.117
112.5	21.4	0.109
112	26	0.101
111.5	34	0.092
111	48	0.081
110	76	0.072

T_c Post-Mortem. In order to evaluate the possibility that the electrochemical experiment might somehow damage the superconductor surface, we performed four-point probe resistivity measurements on a Tl_{2223} superconductor electrode following its use in impedance experiments. Above T_c, the resistance was measurable and gradually decreased with temperature, as expected. Near 112 K, the measured voltage across the two inner Ag lines (i.e., the electrode resistance) dropped abruptly to a value too small to measure. These observations are consistent with the Tl_{2223} electrode specimen having retained its superconductive properties following the electrochemical experiments. We believe therefore that electrolytic damage is minimal or absent in this aprotic low-temperature solvent (in contrast to that possible in acidic media).[2b,9b,c] Electrolytic stability of an oxide surface in an aprotic solvent is not unusual.

High Frequency Results. The high frequency arc yields data on the bulk solvent and shows no sensitivity to the T_c of the electrode or, as noted above, the bias voltage. Our principal focus is on the low frequency C_{DL} and R_{CT} data, and we report some bulk solvent results only for completeness. Examples of typical solution phase capacitance (C_{bulk}) and resistance (R_{bulk}) values obtained from the high frequency impedance data are given in Table I. An Arrhenius plot of log ($1/R_{bulk}$) vs reciprocal temperature gives an activation energy for the solution conductance of 48 kJ mol^{-1}, which is consistent with earlier experiments on this solvent system.[18]

Acknowledgment. This work was supported in part by grants from the Office of Naval Research and the National Science Foundation. We are grateful to Professor Wolfgang J. Lorenz of the University of Karlsruhe (Germany) and to Professor Richard P. Buck of The University of North Carolina at Chapel Hill for helpful suggestions and insightful comments.

Registry No. Bu_4NClO_4, 1923-70-2; $Tl_2Ba_2Ca_2Cu_3O_{10}$, 115866-07-4; $Tl_2Ba_2CaCu_2O_8$, 115833-27-7; ethyl chloride, 75-00-3; butyronitrile, 109-74-0.

(18) McDevitt, J. T.; Peck, S. R. Unpublished results.